Vol 16 No 1, January 2007
1009-1963/2007/16(01)/0179-07

Chinese Physics

© 2007 Chin. Phys. Soc.
and IOP Publishing Ltd

Non-steady interaction of plasma with aircraft in its near wake region*

Hu Tao-Ping(胡涛平)[a)†] and Luo Qing(罗 青)[b)]

[a)] *College of Information Science and Technology, Nanjing Forestry University, Nanjing* 210037, *China*

[b)] *Department of Physics, Nanjing Xiaozhuang College, Nanjing* 210017, *China*

(Received 28 February 2006; revised manuscript received 10 May 2006)

Non-steady interactions between plasmas and aircraft in its near wake region are investigated in detail. Under the non-static limit, a set of equations that describe these interactions are obtained. The results of the numerical simulation show that the cavitons of transverse plasmas are excited and density cavitons appear when the envelope of plasma becomes sufficiently intensive. This is very important for detecting the moving body that has a 'stealth' characteristic.

Keywords: ionosphere, plasma waves, plasma interaction
PACC: 5235P, 5235S, 5240

1. Introduction

The main aim of this paper is to study the interaction that occurs when a conducting body moves through ionosphere at mesothermal speed. Since the successful launching of man-made satellites into near-Earth and especially missiles into outer space, great interest has been aroused in the study of the interaction effects. The early theoretical studies have been devoted to the effects in the vicinity of a body moving through the ionosphere.[1−3] However, as indicated by Al'pert, a serious shortcoming of the theory at that time is the absence of any studies of non-steady-state problems.[4] It is well known that when a conducting body moves in the ionosphere complicated interactions occur between the moving body and the plasma around it, and the body can excite plasma waves and plasma instabilities. In addition, because of the nonlinear effect, high-frequency electromagnetic wave eradiated by the antenna of aircraft will engender electromagnetic solitary waves when it interacts with plasma.[5,6] In fact, a large amplitude solitary wave has been observed.[7] Since these plasma waves and plasma instabilities in the vicinity of a body moving in ionosphere are typically non-steady-state and nonlinear problems, it is very important to consider non-steady-state and nonlinear effects in the study.[8−14]

On the other hand, in order to find out a moving body in space, we usually detect the radar waves reflected by it. But, because of the rapid development of stealth-body material, the reflections of some aircraft to radar wave are weaker and weaker. This makes us increasingly difficult to discover them. In other words, these aircraft have a 'stealth' characteristic that prevents them from being detecting by radar. Therefore, one main purpose of the investigation is to try to find out an effective method to detect the moving body that has a 'stealth' characteristic.[5,6] As we know, the density cavitons generated by the interactions of plasmas with aircraft cannot be concealed. So the 'stealth' aircraft can be traced by detecting these density cavitons if one knows the characteristic of them. It is very useful in national defense.

Since the characteristic dimension of a body moving in the ionosphere, which is usually of the order of one or a few metres, is much smaller than the mean free path $L(L > 10^2$ m) of particles, we should use the kinetic theory to describe the processes in the vicinity of a moving body.[15] On the other hand, a characteristic of the body moving in the ionosphere is its mesothermal speed v_0, which means that $v_{\rm Ti} \ll v_0 \ll v_{\rm Te}$, ($v_{\rm Ti}$ and $v_{\rm Te}$ are the thermal velocities of ions and electrons). Under this condition the equilibrium of electrons is very weakly disturbed by the body, i.e. the kinetic effects for electrons can be neglected. Hence, we can use the hydrodynamical equations to describe electronic behaviour, and the ion distribution function $f_{\rm i}$ should obey the Vlasov

*Project supported by Nanjing Forestry University Foundation, China (Grant No 163070019).
†E-mail: fox_tphu@sina.com

equation. In addition, quasi-neutral approximation is valid because the directed kinetic energy is much larger than the electrostatic potential energy due to electric field effect, and in many of the ionosphere dynamic problems of interest, the geomagnetic field effect is negligible.[2]

First of all, we must obtain a set of non-steady-state and nonlinear equations that describe these interactions. In the static limit, such equations have been obtained,[5] but it is only relevant for the subsound collapse. With increasing time, the super-sound collapse becomes more important. In this paper, we obtain a new set of non-steady-state and nonlinear coupling equations in the non-static limit. The near wake region is numerically simulated, and we present the distributions of electric field and the density of particles in this region.

This paper is organized as follows. In Section 2, based on the hydrodynamical equations for electrons and the Boltzmann equation for ions, we obtain the non-steady-state and nonlinear coupling equations that describe the interaction between a body moving in space and the plasmas in its near wake. In Section 3, the results of numerical simulation are given. Finally, Section 4 presents the discussion and conclusions.

2. Theoretical calculation

The hydrodynamic equations for electrons and the Maxwell equation can be written as follows:

$$\frac{\partial n_{\rm e}}{\partial t}+\nabla\cdot(n_{\rm e}\boldsymbol{v}_{\rm e})=0, \tag{1}$$

$$\frac{\partial \boldsymbol{v}_{\rm e}}{\partial t}+(\boldsymbol{v}_{\rm e}\cdot\nabla)\boldsymbol{v}_{\rm e}=\frac{e}{m_{\rm e}}\Big(\boldsymbol{E}+\frac{1}{c}\boldsymbol{v}_{\rm e}\times\boldsymbol{B}\Big)-\frac{\gamma_{\rm e}T_{\rm e}}{m_{\rm e}n_{\rm e}}\nabla n_{\rm e}, \tag{2}$$

$$\nabla\times\boldsymbol{E}=-\frac{1}{c}\frac{\partial\boldsymbol{B}}{\partial t}, \tag{3}$$

$$\nabla\times\boldsymbol{B}=\frac{1}{c}\frac{\partial\boldsymbol{E}}{\partial t}+\frac{4\pi e}{c}(n_{\rm e}\boldsymbol{v}_{\rm e}-n_{\rm i}\boldsymbol{v}_{\rm i}), \tag{4}$$

$$\nabla\cdot\boldsymbol{B}=0, \tag{5}$$

where n and $\boldsymbol{v}$ are the density and velocity of electrons, subscripts i and e represent ions and electrons respectively, $\gamma_{\rm e}$ is the specific-heat ratio for electrons, and $T_{\rm e}$ is the temperature of electrons in energy units. The other symbols have their usual meanings.

On the basis of the two time-scale approximations, all the field quantities could be decomposed into the fast time-scale and slow time-scale components

$$A=A_{\rm f}+A_{\rm s}, \tag{6}$$

and it would be assumed that the assembly average value of fast time-scale components over the slow time-scale vanish, i.e.

$$\langle A_{\rm f}\rangle=0. \tag{7}$$

The quasi-neutrality condition is valid on a slow time-scale,

$$\langle en_{\rm e}-en_{\rm i}\rangle=0,\quad n_{\rm s}^{\rm e}=n_{\rm s}^{\rm i}=n_{\rm s}. \tag{8}$$

Substituting the corresponding fast and slow components of the field quantities into these equations, one can deduce from Eq.(1) that

$$\frac{\partial n_{\rm s}}{\partial t}+\nabla\cdot(n_{\rm s}\boldsymbol{v}_{\rm s})=0; \tag{9}$$

studying the momentum equation for the electron from Eq.(2), one obtains

$$\frac{\partial\boldsymbol{v}_{\rm s}}{\partial t}+(\boldsymbol{v}_{\rm s}\nabla)\boldsymbol{v}_{\rm s}=\frac{e}{m_{\rm e}}\boldsymbol{E}_{\rm s}-\frac{\gamma_{\rm e}T_{\rm e}}{m_{\rm e}n_{\rm s}}\nabla n_{\rm s}-\frac{1}{2}\nabla\langle(v_{\rm f})^2\rangle, \tag{10}$$

the very weak geomagnetic field has been ignored on the right-hand side of the above equation. By use of Eqs.(2)–(4), we arrive at the equation

$$\frac{\partial^2\boldsymbol{E}_{\rm f}}{\partial t^2}+c^2\nabla\times\nabla\times\boldsymbol{E}_{\rm f}+\omega_{\rm pe}^2\boldsymbol{E}_{\rm f}+\frac{\delta n}{n_0}\omega_{\rm pe}^2\boldsymbol{E}_{\rm f}-\gamma_{\rm e}v_{\rm Te}^2\nabla(\nabla\cdot\boldsymbol{E}_{\rm f})=0, \tag{11}$$

where $\omega_{\rm pe}^2=4\pi n_0e^2/m_{\rm e}$. In the calculations the following condition should be satisfied:

$$W=\frac{|\boldsymbol{E}_{\rm f}|^2}{4\pi n_0T_{\rm e}}\le 1. \tag{12}$$

We introduce the following fields of type Van der Pol:

$$\boldsymbol{v}_{\rm f}=\frac{1}{2}[\boldsymbol{v}(\boldsymbol{r},t){\rm e}^{{\rm i}\omega t}+{\rm c.c.}], \tag{13}$$

$$\boldsymbol{E}_{\rm f}=\frac{1}{2}[\boldsymbol{E}(\boldsymbol{r},t){\rm e}^{{\rm i}\omega t}+{\rm c.c.}], \tag{14}$$

where the amplitudes $\boldsymbol{v}(\boldsymbol{r},t)$ and $\boldsymbol{E}(\boldsymbol{r},t)$ are slowly varying functions over time, c.c. denotes the complex conjugate of the first term. Substituting Eq.(14) into Eq.(11), we obtain the amplitude transport equation of the fast-varying field with $\omega\approx\omega_{\rm pe}$,

$$2{\rm i}\omega_{\rm pe}\frac{\partial\boldsymbol{E}}{\partial t}+c^2\nabla\times\nabla\times\boldsymbol{E}-\gamma_{\rm e}v_{\rm Te}^2\nabla(\nabla\cdot\boldsymbol{E})+\frac{\delta n}{n_0}\omega_{\rm pe}^2\boldsymbol{E}=0. \tag{15}$$

In the above equation, the second partial derivative $\partial^2\boldsymbol{E}/\partial t^2$ has been omitted in the slowly varying approximation. At the same time, Eq.(10) can be transformed into

$$\frac{\partial\boldsymbol{v}_{\rm s}}{\partial t}+(\boldsymbol{v}_{\rm s}\cdot\nabla)\boldsymbol{v}_{\rm s}=-\frac{e}{m_{\rm e}}\nabla\phi-\frac{\gamma_{\rm e}T_{\rm e}}{m_{\rm e}}\frac{\nabla(n_0+\delta n)}{n_0+\delta n}$$

$$-\frac{1}{16\pi n_0 m_\mathrm{e}}\nabla(|\boldsymbol{E}|^2), \tag{16}$$

where $\boldsymbol{E}_\mathrm{s}=-\nabla\phi$. And using Eqs.(9) and (16), we finally have[5]

$$\Big(\frac{\partial^2}{\partial t^2}-\gamma_\mathrm{e}v_\mathrm{Te}^2\nabla^2\Big)\frac{\delta n}{n_0} = \frac{e}{m_\mathrm{e}}\nabla^2\phi+\frac{1}{m_\mathrm{e}}\nabla^2\Big(\frac{|\boldsymbol{E}|^2}{16\pi n_0}\Big). \tag{17}$$

For closing Eqs.(15) and (17), we have to study the influence of the slowly-varying field ϕ on ion flow. In addition, since the body's velocity is considerably greater than the thermal velocity of the ion, a disturbance of the ions occurs basically because of their interactions with the body itself. In a coordinate system moving with the body, the Boltzmann equation for ionic distribution function f_i is of the form

$$\frac{\partial f_\mathrm{i}}{\partial t}+\boldsymbol{v}\frac{\partial f_\mathrm{i}}{\partial \boldsymbol{r}}-e_\mathrm{i}\frac{\partial\varphi}{\partial\boldsymbol{r}}\frac{\partial f_\mathrm{i}}{\partial\boldsymbol{p}}=A_\mathrm{i}(\boldsymbol{r},\boldsymbol{v},t)\delta(F) -\nu\Big(\delta f-\frac{f_0}{n_0}\int\delta f\mathrm{d}^3\boldsymbol{v}\Big), \tag{18}$$

where A_i is the function describing the interaction of plasma with the surface of the aircraft, $F(\boldsymbol{r}_\mathrm{s})=0$ is the surface function of the aircraft, $\boldsymbol{r}_\mathrm{s}$ is the radius of the aircraft, $\boldsymbol{p}$ is the momentum of ions, and ν is the collision frequency of ions.

Let us assume that

$$f_\mathrm{i}=f_0+\delta f,\quad(\delta f\ll f_0), \tag{19}$$

$$f_0=n_0\frac{(2\pi)^{3/2}}{(m_\mathrm{i}v_\mathrm{Ti})^3}\exp\Big(-\frac{\boldsymbol{p}_\mathrm{u}^2}{2m_\mathrm{i}^2v_\mathrm{Ti}^2}\Big), \tag{20}$$

where f_0 is a balance distribution of the undisturbed ions, the normalization of which is

$$n_0=\int f_0\frac{\mathrm{d}\boldsymbol{p}}{(2\pi)^3}. \tag{21}$$

Substituting Eq.(20) into Eq.(18) and using the Fourier transform

$$A(\boldsymbol{r},t)=\int A_{\Omega,\boldsymbol{k}}\exp(-\mathrm{i}\Omega t+\mathrm{i}\boldsymbol{k}\cdot\boldsymbol{r})\mathrm{d}\boldsymbol{k}\mathrm{d}\Omega, \tag{22}$$

$$A_{\Omega,\boldsymbol{k}}=\frac{1}{(2\pi)^4}\int A(\boldsymbol{r},t)\exp(\mathrm{i}\Omega t-\mathrm{i}\boldsymbol{k}\cdot\boldsymbol{r})\mathrm{d}\boldsymbol{r}\mathrm{d}t, \tag{23}$$

as well as to a fixed coordinate system

$$\boldsymbol{u}=\boldsymbol{v}+\boldsymbol{v}_0,\quad \boldsymbol{p}_\mathrm{u}=m_\mathrm{i}\boldsymbol{u}, \tag{24}$$

where $\boldsymbol{v}_0$ is the velocity of the body, one obtains from Eq.(18) that

$$-\mathrm{i}(\Omega-\boldsymbol{k}\cdot(\boldsymbol{u}-\boldsymbol{v}_0))(\delta f)_{\Omega,\boldsymbol{k}}=\mathrm{i}(e_\mathrm{i}\varphi_{\Omega,\boldsymbol{k}})\boldsymbol{k}\cdot\frac{\partial f_0}{\partial\boldsymbol{p}_\mathrm{u}} +I_{\Omega,\boldsymbol{k}}-\nu(\delta f)_{\Omega,\boldsymbol{k}}+\nu\frac{f_0}{n_0}(\delta n)_{\Omega,\boldsymbol{k}}, \tag{25}$$

where

$$I_{\Omega,\boldsymbol{k}}=\Big[\frac{\partial(\delta f)}{\partial\boldsymbol{p}_\mathrm{u}}\cdot\frac{\partial(e_\mathrm{i}\varphi)}{\partial\boldsymbol{r}}\Big]_{\Omega,\boldsymbol{k}}+\int A_\mathrm{i}(\boldsymbol{r},\boldsymbol{v},t)\delta(F) \times\exp(\mathrm{i}\Omega t-\mathrm{i}\boldsymbol{k}\cdot\boldsymbol{r})\frac{\mathrm{d}\boldsymbol{r}\mathrm{d}t}{(2\pi)^4}. \tag{26}$$

The third term on the right-hand side of Eq.(25) can be ignored in far wake region of the aircraft because it is small in that region which corresponds to small values of $\boldsymbol{k}$.[5] But in the near region we cannot ignore it since it is no longer small. Integrating Eq.(25) with respect to $\mathrm{d}\boldsymbol{p}_\mathrm{u}$, we have

$$(\delta n)_{\Omega,\boldsymbol{k}}=I_1+I_2+I_3, \tag{27}$$

where

$$I_1=-e_\mathrm{i}\varphi_{\Omega,\boldsymbol{k}}\int\frac{\boldsymbol{k}\cdot(\partial f_0/\partial\boldsymbol{p})}{\Omega-\boldsymbol{k}\cdot(\boldsymbol{u}-\boldsymbol{v}_0)+\mathrm{i}\nu}\mathrm{d}p_x\mathrm{d}p_y\mathrm{d}p_z =-\frac{e_\mathrm{i}\varphi_{\Omega,\boldsymbol{k}}}{T_\mathrm{i}}\Big[n_0+n_0\frac{\boldsymbol{k}\cdot\boldsymbol{v}_0}{\sqrt{2}kv_\mathrm{Ti}}\mathrm{i}Q(a)\Big], \tag{28}$$

$$I_2=\int\frac{I_{\Omega,\boldsymbol{k}}}{-\mathrm{i}(\Omega-\boldsymbol{k}\cdot(\boldsymbol{u}-\boldsymbol{v}_0)+\mathrm{i}\nu)}\mathrm{d}p_x\mathrm{d}p_y\mathrm{d}p_z =-\frac{\pi R_0^2v_0n_0}{\sqrt{2}kv_\mathrm{Ti}}Q(a), \tag{29}$$

$$I_3=\frac{\nu(\delta n)_{\Omega,\boldsymbol{k}}}{n_0}\int\frac{f_0}{-\mathrm{i}(\Omega-\boldsymbol{k}\cdot(\boldsymbol{u}-\boldsymbol{v}_0)+\mathrm{i}\nu)} \times\mathrm{d}p_x\mathrm{d}p_y\mathrm{d}p_z=-\frac{\nu(\delta n)_{\Omega,\boldsymbol{k}}}{\sqrt{2}kv_\mathrm{Ti}}Q(a), \tag{30}$$

with

$$Q(a)=\Big(\sqrt{\pi}+2\mathrm{i}\int_0^a\exp(x^2)\mathrm{d}x\Big)\exp(-a^2),\qquad a=\frac{1}{\sqrt{2}kv_\mathrm{Ti}}(\boldsymbol{k}\cdot\boldsymbol{v}_0+\mathrm{i}\nu). \tag{31}$$

When $a\ll1$, the second term in the bracket on the right-hand side of the above equation is much smaller than the first one. So, ignoring it, we have

$$Q(a)\approx\sqrt{\pi}\exp(-a^2). \tag{32}$$

The expression in Eq.(29) is I-function defined by Al'pert *et al.* It is proportional to the number of ions that have momentum $\boldsymbol{p}_\mathrm{u}$ due to the scattering between aircraft and the field around it during unit time. I-function is usually determined by the interaction between aircraft and plasma around it. If the scattering is mirror-image symmetrical i.e. if the angle of incidence of the particle on the surface is equal to its angle of reflection, then we have

$$I_{\Omega,\boldsymbol{k}}\approx-\pi R_0^2v_0f_0. \tag{33}$$

R_0 is the radius of the aircraft (assume that the shape of aircraft is spherical). For this case of low frequency, i.e. $\Omega \ll \boldsymbol{k}\cdot(\boldsymbol{u}-\boldsymbol{v}_0)$, we ignore Ω in the denominators of the integral equations. Then, we obtain

$$\Big[1+\frac{\nu}{\sqrt{2}kv_{\rm Ti}}Q(a)\Big]\frac{\delta n}{n_0}=\frac{e\varphi}{T_{\rm i}}-\frac{\pi R_0^2 v_0}{\sqrt{2}kv_{\rm Ti}}Q(a). \tag{34}$$

By use of Eqs.(34) and (17), eliminating φ, we have

$$\begin{aligned}&\Big[\frac{\partial^2}{\partial t^2}-(\gamma_{\rm e}v_{\rm Te}^2+\frac{T_{\rm i}}{m_{\rm e}}A)\nabla^2\Big]\frac{\delta n}{n_0}\\&\quad=\frac{T_{\rm i}}{m_{\rm e}}\nabla^2 B+\frac{1}{m_{\rm e}}\nabla^2\Big(\frac{|E|^2}{16\pi n_0}\Big),\end{aligned} \tag{35}$$

where

$$A=1+\frac{\nu}{\sqrt{2}kv_{\rm Ti}}Q(a),\quad B=\frac{\pi R_0^2 v_0}{\sqrt{2}kv_{\rm Ti}}Q(a). \tag{36}$$

In terms of the dimensionless variables

$$\begin{aligned}&\boldsymbol{r}'=\frac{2}{3}\frac{\omega_{\rm pe}}{c_{\rm s}}\mu\boldsymbol{r},\quad \tau=\frac{2}{3}\mu\omega_{\rm pe}t,\quad n=\frac{3}{4\mu}\frac{\delta n}{n_0},\\&\boldsymbol{E}'=\frac{\sqrt{3}\boldsymbol{E}}{8[\pi n_0\mu(\gamma_{\rm e}T_{\rm e}+T_{\rm i})]^{1/2}},\quad \boldsymbol{v}'_0=\frac{\boldsymbol{v}_0}{c_{\rm s}},\\&\mu=\frac{m_{\rm e}}{m_{\rm i}},\quad \alpha=\frac{c^2}{3v_{\rm Te}^2},\quad c_{\rm s}^2=\frac{T_{\rm e}}{m_{\rm i}},\end{aligned} \tag{37}$$

Eqs.(15) and (35) may be written as

$$\mathrm{i}\frac{\partial \boldsymbol{E}'}{\partial t}+\alpha\nabla\times\nabla\times\boldsymbol{E}'-\nabla(\nabla\cdot\boldsymbol{E}')+n\boldsymbol{E}'=0,$$

$$\Big[\frac{\partial^2}{\partial t^2}-\Big(\gamma_{\rm e}+\frac{T_{\rm i}}{T_{\rm e}}A\Big)\nabla^2\Big]n \tag{38}$$

$$=\frac{3}{4\mu}\frac{T_{\rm i}}{T_{\rm e}}\nabla^2 B+\Big(\gamma_{\rm e}+\frac{T_{\rm i}}{T_{\rm e}}\Big)\nabla^2|\boldsymbol{E}'|^2. \tag{39}$$

Thus, we have the nonlinear coupling equations (i.e. Eqs.(38) and (39)) describing the high-frequency field and density disturbance in the near wake region. We should notice that Eqs.(38) and (39) are only valid under the condition of $W\le 1$.

3. Numerical simulation

We can obtain the distributions of $\boldsymbol{E}'$ and n by numerically calculating Eqs.(38) and (39). And the electric field $\boldsymbol{E}'$ may be taken in two dimensions with three components because the near-wake region of the moving body is symmetrical about the direction $\boldsymbol{v}_0$ of the aircraft. The purpose of the choice enables us to calculate all the field quantities with the numerical simulation method. We use FTCS (time forward-difference and space central-difference method) as the numerical method. Meanwhile, the periodic boundary condition in the z direction is used in the numerical simulation. In the r direction in the calculation, the natural boundary condition has been used, i.e. the field quantities are zero when $r\to\infty$. Because the amplitude of the high-frequency electric field radiated by an antenna has the form of an envelope, and the radiation is strong transverse plasma wave, we can consider it to be the effect of transverse wave. In a cylindrical coordinate system, the initial condition is chosen as

$$\begin{aligned}\boldsymbol{E}'(\boldsymbol{r},\tau=0)&=E_0\sin\Big(\frac{2\pi z}{z_0}\Big)\exp\Big(-\frac{r^2}{r_0^2}\Big)\boldsymbol{e}_r\\&+E_0\sin\Big(\frac{2\pi z}{z_0}\Big)\exp\Big(-\frac{r^2}{r_0^2}\Big)\boldsymbol{e}_\varphi\\&+E_0\Big[\frac{z_0}{2\pi r}-\frac{z_0 r}{\pi r_0^2}\Big]\cos\Big(\frac{2\pi z}{z_0}\Big)\exp\Big(-\frac{r^2}{r_0^2}\Big)\boldsymbol{e}_z.\end{aligned} \tag{40}$$

Equation (40) represents a very slowly varying vector field, and has the form of travelling transverse envelope, where z, z_0, r and r_0 are dimensionless variables. Although Eq.(40) is not the same as the real electric field, it enables us to obtain more realistic results because it has a similar form to the real electric field. In addition, the choice of an initial wave field (40) can reduce the time of field collapse. On the other hand, because the field has the axially symmetrical property, the initial condition should be axially symmetrical, and the case $r=0$ should be excluded. The choice of the initial condition is based on the consideration of this fact. In Eq.(40), $z_0=50$ and $r_0=10$ are the widths of the wave packet of the electric field. The initial condition satisfies the condition for a transverse wave $\nabla\cdot\boldsymbol{E}'(r,\tau=0)=0$, and has $|\boldsymbol{E}'|^2_{\max}(\tau=0)=6.38$. The spatial range of the numerical simulation is chosen as $\Delta z=50$ and $\Delta r=25$, their dimensional values are $\Delta z\approx 40$ m and $\Delta r\approx 20$ m. The dimensionless distance between the back surface of the moving body and the simulation space is $L_0=1$, which corresponds to a dimensional value about $L_0\approx 0.8$ m. The parameters of the moving body and the ionosphere are chosen as $v_0=10^6$ cm/s, $R_0=100$ cm, $T_{\rm i}=T_{\rm e}=3000$ K, $n_{\rm e}=10^5/\ {\rm cm}^3$, $\nu=0.1\ {\rm sec}^{-1}$ and $E_0=1.8$. From the electron temperature, it is easy to obtain the parameter $\alpha=6.6\times10^5$. The solutions of Eqs.(38) and (39) with this initial condition are shown in Figs.1 and 2 respectively. We have used the expressions $\tau=\tau_n\times\delta\tau$, step $\delta\tau=0.000005$ and the dimensionless quantity $W=|\boldsymbol{E}_{\rm f}|^2/4\pi n_0 T_{\rm e}$ defined in Eq.(12).

4. Conclusion and discussion

The distributions of the collapses of electric field and density cavitons are shown respectively in Figs.1 and 2. The distributions indicate that the growth rates of the perturbation in the whole space of the numerical simulation are different and the growth rates at the peaks of collapses are larger. From Fig.1, we can see that with increasing time, the intensity of the electric field around some certain place becomes larger and larger. At the same time, the spatial range of the field becomes smaller and smaller, leading to collapses and cavitons. This conclusion is qualitatively the same as the analysis of Ref.[5]. On the other hand, the collapses of the field result in the formation of density cavitons in the near wake region. Since the cavitons and the density cavitons are generated by the interaction between the aircraft and the plasma around it, we can find the 'stealth' aircraft by detecting them.

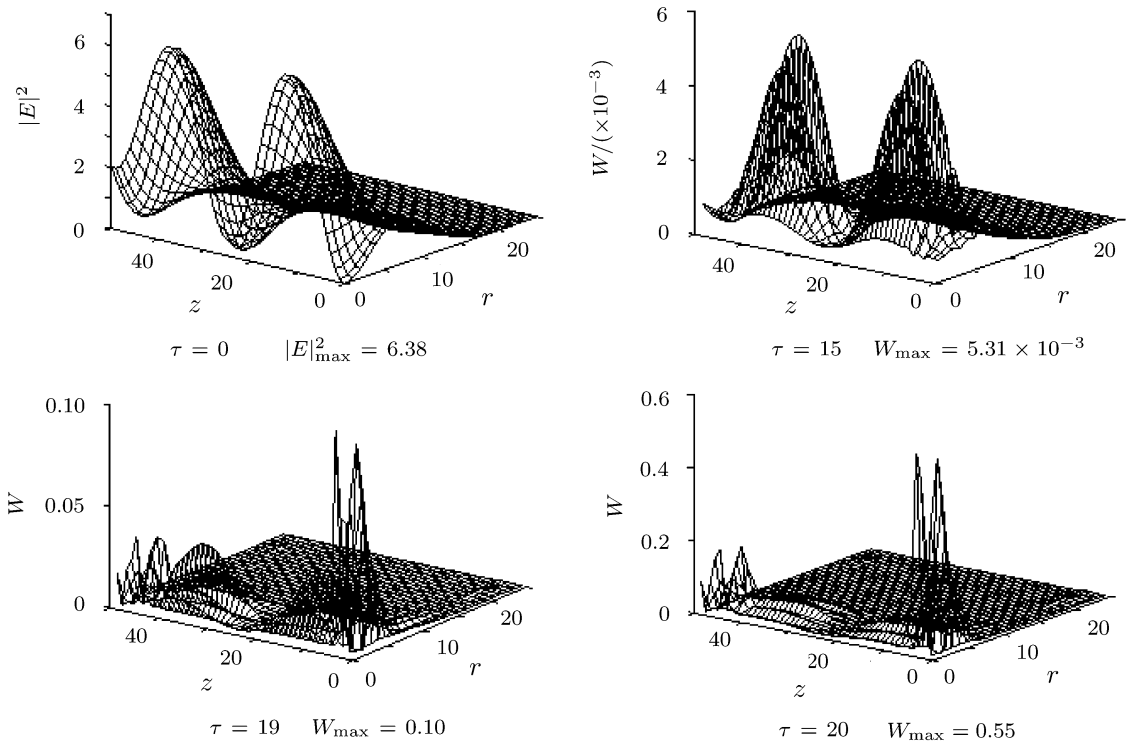


Fig.1. Collapse evolution of electric field $W = |\boldsymbol{E}_{\rm f}|^2/4\pi n_0 T_{\rm e}$.

It can be seen from Eq.(38) that the density disturbance, the derivative of the field and the intensity of the field can influence the collapse pattern. At first, because the intensity of the field is small, the locations of the collapse peaks are mainly determined by the density disturbance and the gradients of the field. But with increasing time, the magnitude of the field determines the values of the collapse peaks. In Fig.1, the rapid augment of the intensity of the field in the collapse peak proves this point.

In Eq.(39), $|\boldsymbol{E}'|^2$ of the second term of the density disturbance on the right-hand side comes from the ponderomotive force of the high-frequency field. This term indicates that the maximum disturbance of the density occurs at the location where the intensity of the field is maximal. From Fig.2, we know that the effect of the nonstandard term is at first larger than the ponderomotive force term. At that time, the speed of collapse is slow because it is sub-sound collapse. With increasing time, the influence of the ponderomotive force becomes more and more important, and the speed of collapse becomes fast because it becomes super-sound collapse.

The numerical results show that the envelope field

itself suffers collapse, leading to localization of the field. This means that when time increases, the intensity of field becomes stronger and stronger, and the range of the field is smaller and smaller at the locations of collapse peaks. However, we should note that the numerical calculation does not go on forever. When the evolution time is larger than a certain value, the field collapses rapidly. This leads to the formation of a very strong field in which the condition $W \leq 1$ is not valid. This particular value of the evolution time corresponds to $\tau_n = 20$ in our calculation, and we stop our calculation there. In addition, when $W > 1$, stronger turbulent interactions occur between field and particles. The field energy will be transferred to the particles through the interactions. Since the particle energy (i.e. $k_{\mathrm{B}}T_{\mathrm{e}}$) increases and the field energy decreases, W will decrease until the condition $W \leq 1$ is satisfied again. The time of the stronger turbulent interactions, compared with the weaker interaction, is very short.

Finally, we indicate that for a transverse plasma wave, because its group velocity is much smaller than the velocity of light, it is not easy for it to escape from the source region. This enables the wave to collapse through interactions between the wave and the particles. On the other hand, considering the above discussion, the choice of initial condition (40) is not unique. The amplitude of any propagating transverse wave that is a slowly varying function of time can be chosen as the initial condition if it satisfies the condition for a transverse wave. Different initial conditions may lead to different locations of the collapse peaks (different collapse patterns). The collapse velocity may be different: fast or slow. However, the collapse tendency of the envelope field is similar. In addition, although the main conclusions can be given in a two-dimensional subspace, the numerical simulations that are obtained in three dimensions with three field components are more realistic than the above results. However, it is very difficult to realize the simulation in a three-dimensional space due to the great quantity of calculation required.

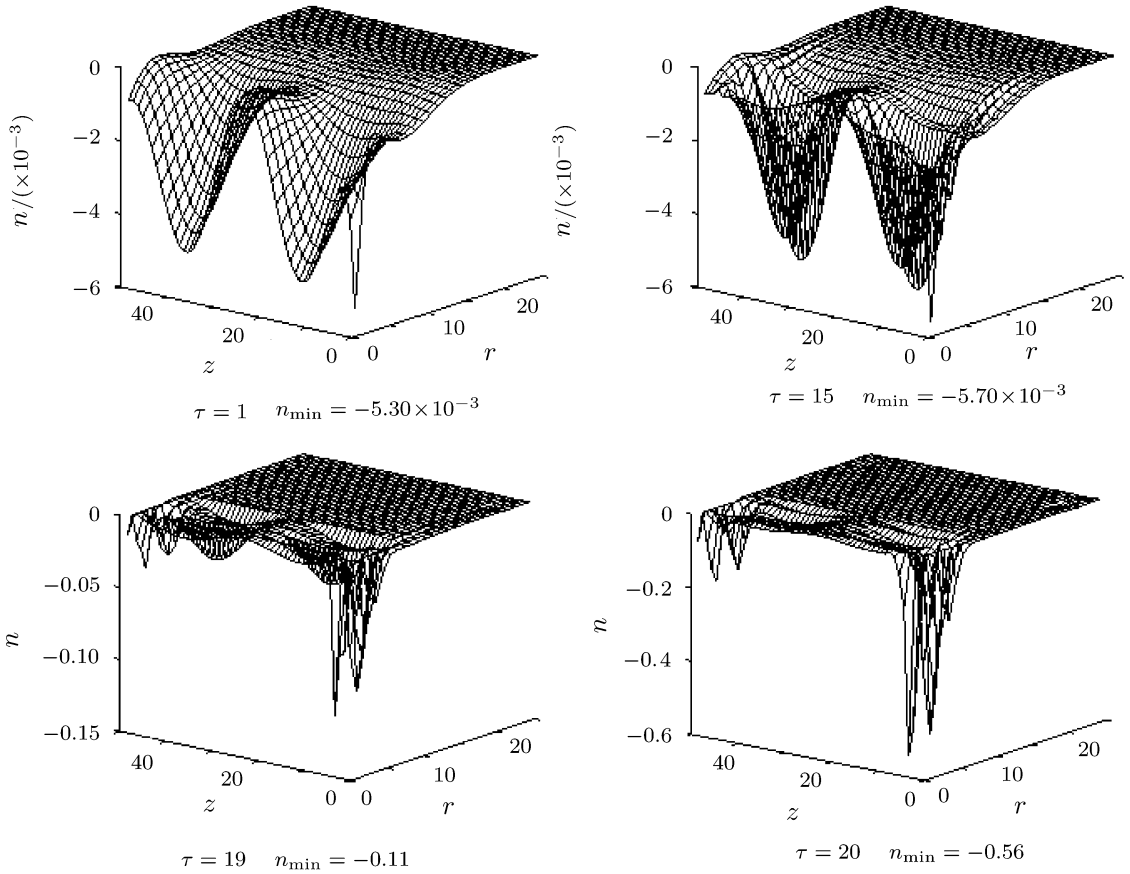


Fig.2. Collapse evolution of density of particles.

References

[1] Al'pert Y, Gurevich A V and Pitaevskii L P 1965 *Space Physics with Artificial Satellites* (New York: Plenum)

[2] Liu V C 1969 *Space Sci. Rev.* **9** 423

[3] Gurevich A V, Pitaevskii L P and Smirnova V V 1969 *Space Sci. Rev.* **9** 805

[4] Al'pert Y 1983 *The Near-Earth and Interplanetary Plasma* (Cambridge: Cambridge University Press)

[5] Li X Q 1993 *Progress in Physics* **13** 595 (in Chinese)

[6] Li X Q 1990 *Acta Aeronautics and Space Sin.* **3** 76 (in Chinese)

[7] Bakai A S, Kuperov L P and Solodovnikov G K 1977 *Soviet J. Plasma Phys.* **3** 572

[8] Zhang J Q, Liang C H, Wang G G and Zhu J Z 2003 *Acta Phys. Sin.* **52** 890 (in Chinese)

[9] Huang D J and Zhang H Q 2004 *Acta Phys. Sin.* **53** 2435 (in Chinese)

[10] Biasca R and Wang J 1995 *Phys. Plasmas* **2** 280

[11] Wang Y Y, Yang Q, Dai C Q and Zhang J F 2006 *Acta Phys. Sin.* **55** 1029 (in Chinese)

[12] Hu Q L and Liu S B 2005 *Chin. Phys.* **14** 2546

[13] Dobrowolny M, Dobrowolny R, Vannaroni G and De Venuto F 1998 *Il Nuovo Cimento.* **21** 85

[14] Enloe C L, Cooke D L, Pakula W A, Violet M D, Hardy D A, Chaplin C B, Kirkwood R K, Tautz M F, Bonito N, Roth C, Courtney G, Davis V A, Mandell M J, Hastings D E, Shaw G B, Giffin G and Sega R M 1997 *J. Geophys. Res.* **102** 425

[15] Li X Q 2004 *Plasma Collapse Dynamics* (Beijing: Chinese Science and Technology Press)